LLNL-CONF-703328

Ion Kinetic Dynamics in Strongly-Shocked Plasmas Relevant to ICF

H. G. Rinderknecht, P. A. Amendt, M. J. Rosenberg, C. K. Li, J. A. Frenje, M. Gatu Johnson, H. Sio, F. H. Seguin, R. D. Petrasso, A. B. Zylstra, G. Kagan, N. M. Hoffman, S. Wilks, V. Yu Glebov, C. Stoeckl, T. C. Sangster

September 20, 2016

26th IAEA Fusion Energy Conference
Kyoto, Japan
October 17, 2016 through October 22, 2016

Ion Kinetic Dynamics in Strongly-Shocked Plasmas Relevant to ICF

H. G. Rinderknecht[1], P. A. Amendt[1], M. J. Rosenberg[2], C. K. Li[3], J. A. Frenje[3], M. Gatu Johnson[3], H. Sio[3], F. H. Séguin[3], R. D. Petrasso[3], A. B. Zylstra[4], G. Kagan[4], N. M. Hoffman[4], S. Wilks[1], V. Yu. Glebov[2], C. Stoeckl[2] and T. C. Sangster[2]

[1]Lawrence Livermore National Laboratory, Livermore, California 94550
[2]Laboratory for Laser Energetics, University of Rochester, Rochester, New York 14623
[3]Plasma Science and Fusion Center, Massachusetts Institute of Technology, Cambridge, Massachusetts 02139
[4]Los Alamos National Laboratory, Los Alamos, New Mexico 87545

Corresponding Author: rinderknecht1@llnl.gov

Abstract:

Implosions of thin-shell capsules produce strongly-shocked ($M > 10$), low-density ($\rho \sim$ 1 mg/cc), high-temperature ($T_i \sim$ keV) plasmas, comparable to those produced in the strongly-shocked DT-vapor in inertial confinement fusion (ICF) experiments. A series of thin-glass targets filled with mixtures of deuterium and Helium-3 gas ranging from 7% to 100% deuterium was imploded to investigate the impact of multi-species ion kinetic mechanisms in ICF-relevant plasmas over a wide range of Knudsen numbers ($N_K \equiv \lambda_{ii}/R$). Anomalous trends in nuclear yields and burn-averaged ion temperatures in implosions with $N_K > 0.5$, which have been interpreted as signatures of ion species separation and ion thermal decoupling [H. G. Rinderknecht et al., Phys. Rev. Lett. 114, 025001 (2015)], are found not to be consistent with single-species ion kinetic effects alone. Experimentally-inferred Knudsen numbers predict an opposite yield trend to those observed, confirming the dominance of multi-species physics in these experiments. In contrast, implosions with $N_K \sim 0.01$ follow the expected yield trend, suggesting single-species kinetic effects are dominant. The impact of the observed kinetic physics mechanisms on the formation of the hotspot in ICF experiments is discussed.

1 Introduction

Understanding the evolution of the plasma during the shock transit phase is fundamentally important for achieving ICF ignition, because the shock sets the initial conditions for hotspot formation, compression, ignition and burn.[1] In the current ignition design for ICF, four shocks compress the cryogenic deuterium-tritium (DT) fuel, then combine into a single strong shock with Mach number ∼10–50.[2] This strong shock transits the central gas, a DT-vapor with initial density 0.3 mg/cc, and converges at the center of the implosion. However the plasma produced by the shock transit is both relatively low in density and high in temperature, because strong shocks compress a plasma only up to a constant factor but heat the plasma proportionally to M^2. These conditions produce long ion-ion mean-free-paths, which scale as $\lambda_{ii} \propto T^2/n \propto M^4$. Quantitatively, the ion-ion mean-free-paths in the shocked central plasma reach $\lambda_{ii} \approx 100$ μm, which is comparable to the scale size of the experiment.[3] Such conditions are precisely those in which the hydrodynamic assumptions begin to break down and kinetic physics becomes important. Kinetic physics has been observed to impact the evolution and nuclear performance of multi-species plasmas in computational studies,[4, 5, 6] although no fully kinetic model is yet capable of simulating an entire ICF implosion.

ICF experiments are generally designed using radiation-hydrodynamic simulations that iteratively solve the equations of motion for a single ion-species plasma. Recent implosions varying the density of the fuel demonstrated that such simulations increasingly overpredict the nuclear observables (e.g. fusion yield, ion temperature) as the ion-ion mean-free-path in the fuel during burn increases.[7, 3] Defining the Knudsen number as the ratio between the average ion-ion mean-free-path and the hot-spot radius during peak nuclear production, $N_K = \langle\lambda_{ii}\rangle/R$, the nuclear yield was reduced relative to the hydrodynamic predictions by a factor of $\sim 0.1/N_K$, for $N_K > 0.1$. This effect was reasonably explained by two effects associated with the ion mean-free-path: the direct reduction of the fusion reactivity by the loss of the energetic tail ions which dominate fusion;[8, 9, 10] and the dilution and loss of fuel from the core due to ion diffusion into the shell plasma during the implosion.[7, 11]

Recent experimental[12, 13, 14, 15, 16] and theoretical work[17, 18, 19, 20, 21, 4, 5] has also investigated the impact of multiple ion species on ICF implosions. Deuterium-^{3}He gas-filled implosions relevant to the shock phase of ICF have demonstrated that simulations increasingly overpredict the nuclear yield as the fraction of ^{3}He in the fuel is increased.[16]. For high-density implosions with moderate Knudsen numbers ($N_K \lesssim 1$), diffusive separation of the ion species was found to be dominant. Low-density implosions ($N_K \sim 10$) demonstrated evidence of thermal decoupling between the two ion species.

The effects of long mean-free-paths and multiple ion species have so far been studied separately. However, because the mean-free-path for a given ion depends upon the charge and mass of all species in the plasma, the effects long mean-free-paths will couple to ion concentration. The mean-free-path for an ion of species j interacting with species k is given by the formula:

$$\lambda_{j,k} = \frac{3}{4\pi}\left(\frac{4\pi\epsilon_0}{e^2 Z_j Z_k}\right)^2 \frac{T^2 m_j}{n_k m_r \ln\Lambda}, \tag{1}$$

where $Z_{j,k}$ are the ionization states, $m_{j,k}$ the ion masses and m_r the reduced mass, T the ion temperature of both species, n_k the field ion density, and $\ln\Lambda$ the Coulomb logarithm. When multiple species are present, the total mean-free-path for species j is the inverse sum of the mean-free-path relative to all species: $\lambda_j = \left[\sum_k \lambda_{j,k}^{-1}\right]^{-1}$. The mean-free-path for different species therefore remain distinct regardless of the concentration, such that any effects due to long mean-free-paths will impact each species separately. Moreover, the average mean-free-path can vary strongly with the ion concentration, if species with different charges are present. For example, assuming thermalized ion species and ignoring variations in the Coulomb logarithm, the scaling of the mean-free-path for deuterons and ^{3}He in a plasma with constant mass density ρ can be calculated as a function of the deuterium fraction, $f_D \equiv n_D/(n_D + n_{^3He})$:

$$\lambda_D = \frac{10\,(3 - f_D)}{(24 - 19 f_D)}\lambda_C, \qquad \lambda_{^3He} = \frac{5\,(3 - f_D)}{8\,(5 - 4 f_D)}\lambda_C, \tag{2}$$

where the constant of proportionality $\lambda_C = (3/4\pi)(4\pi\epsilon_0/e^2)^2 T^2 m_p/(\rho \log \Lambda)$. While the deuteron mean-free-path is always 3.3× that of a ^{3}He ion to within 5%, the mean-free-path for each species increases by greater than 3× as f_D increases from 0 to 1.This reduced confinement with increasing deuterium fraction stems primarily from the decrease in average field ion charge ($\lambda_{ii} \propto \langle Z \rangle^{-2}$), partially balanced by an increase in the ion number density as the mass density is held constant. An average mean-free-path for the plasma, calculated by weighting the species-specific mean-free-paths by their relative concentration, is more than a factor of 10 greater for the pure deuterium plasma than for pure ^{3}He. Because of this strong dependence of N_K on f_D, experimental studies must be careful to distinguish between observed trends due to the (in principle) "single-species" effects of large N_K and the multi-species effects dependent on f_D.

Data from D^{3}He-gas filled implosions with low and high Knudsen numbers and varying deuterium fraction illuminate the interaction of the two previously studied classes of kinetic phenomena – long mean-free-path effects and multi-species effects – and demonstrate that different physics dominates the observed nuclear performance trends in the low- and high-N_K regimes. In this paper, Section 2 describes the design of experiments to probe kinetic fuel dynamics as a function of Knudsen number and fuel concentration. The results are presented in Section 3 and discussed in Section 4. Finally, the relevance of these results to ICF hotspot formation is discussed in Section 5.

2 Experimental Design

The experiments were performed in two campaigns at the 60-beam OMEGA laser facility.[22] In the first campaign, spherical glass capsules with a diameter of 860 μm, a wall thickness of 2.2 μm, and glass density of 2.15 g/cm^3 were filled with various concentrations of D_2 and ^{3}He gas. The atomic deuterium fraction [$f_D \equiv n_D/\,(n_D + n_{^3He})$] of the gas fills ranged from 1 (pure deuterium) to 0.07 (^{3}He-rich), while maintaining a constant initial mass density of $\rho_0 = 0.4$, 1.5, or 3.3 mg/cc.The capsules were imploded by direct laser drive, using a laser pulse with 23 TW peak power and either 0.6 ns (low, high density) or 1.0 ns (mid density) duration. These implosions produced hot ($\langle T_i \rangle \sim$ 10–20 keV) plasmas with low ion density, generating extremely kinetic conditions, with Knudsen numbers in the range $N_K \sim$ 0.5–20.

In the second campaign, gold hohlraums with 1.6 mm diameter, 2 mm length, and 0.8 mm diameter laser entrance holes were used to indirectly drive thin glass shell targets filled with either pure deuterium or 50:50 D:^{3}He-gas. The capsules had an outer diameter of 625 μm, 5.1 μm thick walls, and a fill gas density of 6.1 mg/cm^3. Forty beams containing

17.6 kJ in a 1 ns square impulse drove the hohlraums. Due to the reduced efficiency of indirect drive and the increased gas density, these implosions produced cooler ($\langle T_i \rangle \sim 2$–6 keV), denser plasmas with Knudsen numbers on the order of $N_K \sim 0.01$.

In both series of experiments, the shell burns through prior to shock rebound and the compression of the fuel by remaining shell mass is minimal. For this reason the experiments probe the shock-phase dynamics of plasmas relevant to the central DT-plasma at the beginning of the deceleration phase in laser-driven ICF designs. By comparing the results of experiments in which the Knudsen number ranges from 0.01–10 and the deuterium fraction from 0.07–1.0, the relative importance and impact of mean-free-path scale effects (such as the Knudsen tail ion loss) and multi-species effects (such as ion species separation and thermal decoupling) is studied.

3 Experimental Results

Comprehensive nuclear diagnosis was performed to study the fuel dynamics in these implosions. For all experiments, yields of DD-fusion neutrons (2.45 MeV) were measured using the neutron Time-of-Flight (nTOF) diagnostic suite.[23] Yields and spectra of D^3He-fusion protons (14.7 MeV) were recorded using the Wedge-Range-Filter proton spectrometers (WRF), as well as the Charged Particle Spectrometers (CPS1 and CPS2) for the direct-drive implosions only.[24] Burn-averaged ion temperatures $\langle T_i \rangle$ were inferred from the spectral widths of the nuclear products, after correcting for instrumental broadening.[25, 26] For the low- and high-density direct-drive implosions, the spatial burn profiles of D^3He-protons and DD-protons (3.0 MeV) were measured by penumbral imaging.[27] The shell trajectory was recorded using time-resolved self-emission x-ray imaging.[28] The measured yields and ion temperatures are shown in Table I.[1]

1D-radiation hydrodynamic simulations of the direct-drive implosions were performed using the code HYADES[29] for comparison to the observed values. The simulations were constrained using the measured laser absorption fraction (57%)[30] and DD-neutron and D^3He-proton nuclear-bang times ($\sim$760 and 840 ps, respectively).[31, 32] The indirect-drive implosions were simulated using a radiation-hydrodynamic code, constrained using the hohlraum radiation drive as measured by the DANTE diagnostic,[33] which recorded a peak radiation temperature of $\sim$244.8$\pm$1.4 eV, and the nuclear bang-time (0.92$\pm$0.1 ns) as measured by the particle Time of Flight diagnostic (PTOF).[34]

The reduction in yield relative to 1D as a function of fuel density in similar shock-driven experiments has been described previously;[7, 3] to study the trends with deuterium fraction it is convenient to examine the ratio of measured to simulated yields ("Yield-over-clean" or YOC), as shown in Fig. 1. The direct- and indirect-drive campaigns exhibit clear, opposite trends in YOC with the deuterium fraction: while the direct-drive implosion performance is reduced with smaller f_D, the indirect-drive implosion performance is reduced with greater f_D. The trends in the direct-drive data were explained previously by two effects: separation of the ion species by diffusion in the high-density implosions,

[1] The yield and temperature data from the low- and high-density direct-drive implosions were first reported in Ref. [16].

TABLE I: Experimental nuclear yields, burn-averaged temperatures, and inferred Knudsen numbers (averaged over # shots).

Density mg/cc	f_D	# shots	Yields DD-n	Yields D^{3}He-p	$\langle T_i \rangle_{DDn}$ keV	N_K
6.08	1	3	(4.9±0.4)e8		2.6±0.4	0.050±0.017
(Indirect)	0.5	3	(1.7±0.2)e8	(6.8±0.4)e6	2.9±0.9	0.018±0.010
3.29	1	2	(2.1±0.2)e11		10.8±0.4	
	0.8	1	(1.2±0.1)e11	(2.6±0.3)e10	10.9±0.5	1.16±0.19
	0.5	2	(2.3±0.2)e10	(3.0±0.2)e10	11.9±0.6	0.69±0.11
1.45	1	3	(1.7±0.2)e11		12.0±0.6	1.30±0.67
	0.46	3	(1.8±0.2)e10	(3.8±0.6)e10	13.3±0.6	0.42±0.12
	0.07	4	(3.5±0.5)e8	(8.7±0.8)e9	14.2±2.3	0.22±0.08
0.39	1	3	(3.2±0.6)e10		18.6±0.4	18.5±3.8
	0.8	1	(2.0±0.2)e10	(2.5±0.2)e10	18.5±0.5	9.4±1.4
	0.5	2	(5.1±0.3)e9	(2.5±0.2)e10	17.6±1.7	5.1±2.2
	0.2	2	(7.0±1.1)e8	(1.2±0.2)e10	19.3±2.1	4.1±0.6

and thermal decoupling of the ion species in the low-density implosions.[16] The contrasting trend suggests that neither of these effects dominates the loss of performance in the indirect-drive implosions, and another explanation is required.

The dominant difference between these campaigns is the collisionality of the fuel, which is quantified by the Knudsen number. A "burn-averaged Knudsen number" $\langle N_K \rangle \equiv \langle \lambda_{ii} \rangle / R_{burn} \propto \langle T_i \rangle^2 / \langle n_i \rangle R_{burn}$ may be calculated using the measured burn-average temperatures, radial convergence, and the inferred fuel density during burn $\langle n_i \rangle$.For eight low- and two high-density direct-drive implosions, a burn-average ion density was calculated from the measured nuclear yield, temperature, burn-history and burn volume data, as described in Ref. [16]. On the mid-density direct-drive campaign, since penumbral images were not recorded, the density of the $f_D = 1$ implosions was calculated using the inferred areal density at burn ρR_{burn} from the secondary D-T and D-^{3}He fusion yield,[35, 36] assuming that density scales with convergence cubed. For the remainder of the mid-density shots, the density was calculated assuming the same average convergence as for the deuterium shots. On the indirect-drive campaign, yields were too low to record nuclear images. Instead, the radius at bang-time $R_{bang} \sim 230$ μm was inferred from self-emission x-ray radiographs, and the density was calculated from the initial density $n_{i,0}$ using the scaling relation: $\langle n_i \rangle = n_{i,0}(R_{bang}/R_0)^3$. These calculated values are shown in Figure 2 for each shot; average quantities are listed in Table I. The theoretical trend of $\langle N_K \rangle$ with f_D is calculated using Eqns. 2 and fits are included in Fig. 2; the predicted trends match well the trends in the experimental data.

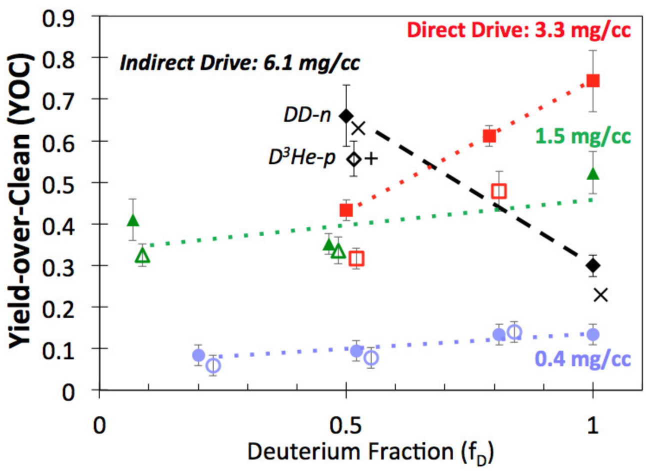

FIG. 1: Measured nuclear yields divided by simulated yield ("Yield-over-clean") for direct-drive implosions with fuel density 3.3 (red □), 1.5 (green △), and 0.4 mg/cc (blue ○), and for indirect-drive implosions with fuel density 6.1 mg/cc (black ◇). Solid indicates DD-neutrons; open, D^3He-protons. Calculated volume-averaged Knudsen reactivity reduction for DD-n (×) and D^3He-p (+) in the indirect-drive implosion conditions are shown. Dashed lines are included to guide the eye.

4 Discussion

Based on Knudsen-layer theory, pure deuterium implosions would be expected to underperform compared to the D^3He-filled implosions: Equation 2 predicts the deuterium Knudsen number to increase by a factor of 2.32× from $f_D = 0.5$ to pure deuterium, or from $N_K \sim 2.2\%$ to $\sim 5.0\%$ based on the values inferred from data. This predicted trend is observed in the indirect-drive implosions.

To estimate the impact of Knudsen-layer tail ion loss on the yields in these experiments, the spherical geometry must be taken into account. The values of $\langle N_K \rangle$ shown in Fig. 2 are for the center of the plasma, but the local Knudsen number (and associated reactivity reduction) will in general be larger as the bulk of the plasma volume is closer to the wall. The volume-averaged reactivities in the conditions of the indirect-drive experiments was calculated using the modified distribution functions presented in Ref. [9] and assuming a uniform spherical plasma in which the local Knudsen number scales inversely with distance to the nearest boundary.[10] This calculation indicates that the volume-averaged reactivity is reduced from 63% of the Maxwellian reactivity for the 50:50 D:^{3}He case to 23% for the pure deuterium. The calculated result is in good agreement with the observed yields-over-clean, as shown in Fig. 1, suggesting that Knudsen-layer reactivity reduction is the dominant effect producing the observed trends in the low-N_K experiments. Note that the reduction with increased f_D is accentuated by the changing composition of the background plasma, which affects the shape of the modified distribution functions.

In contrast, the opposite trend is observed in the direct-drive data, for which the implosions with increased deuterium perform better than D^3He mixtures. In previous work, these trends have been successfully explained by diffusive separation of the fuel

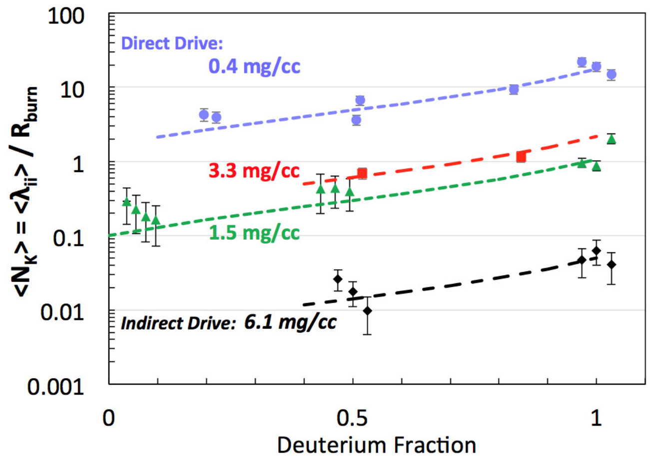

FIG. 2: Inferred burn-averaged Knudsen numbers for direct-drive implosions with fuel density 3.3 (red □), 1.5 (green △), and 0.4 mg/cc (blue ○), and for indirect-drive implosions with fuel density 6.1 mg/cc (black ◇); points spread out for clarity. Knudsen numbers increase with deuterium fraction in agreement with theory (dashed lines; absolute value fit to data). The indirect-drive implosions are substantially more hydrodynamic than direct-drive due to reduced energy coupling to the fuel.

ion species for the high-density case, and thermal decoupling of the ion species in the low-density case.[16] Those explanations stand, however it is important to consider why they dominate over the long mean-free-path mechanisms in the high-N_K experiments. The reactivity reduction formalism is perturbative in the suprathermal ions, and strictly valid only in the regime $N_K \ll 1$. When mean free paths become comparable to the size of the fuel, fusion is no longer dominated by thermal processes, but rather by the density and velocity of the radially-streaming bulk ion populations. As such, the Knudsen number loses relevance as a metric for fusion reactivity. Instead, processes that modify the plasma conditions prior to burn dominate the fusion output. These include ion species separation, which concentrates ^{3}He relative to D in the fuel during the implosion phase; and thermal decoupling of the D and ^{3}He in the shock, which alters the energy balance between these two species. Both of those multi-species effects reduce the performance of mixtures relative to pure fuels, as shown in the data.

5 Conclusion

Nuclear data from D^{3}He-gas filled implosions with varying Knudsen number and deuterium fraction demonstrate a change in the regime of dominant kinetic physics impacting the nuclear performance. Long mean-free-path effects, such as tail-ion-loss, dominate for low Knudsen numbers ($N_K \sim 0.01$), while multi-species effects dominate for high Knudsen numbers ($N_K \gtrsim 0.5$). This suggests that there exists an intermediate Knudsen-number ($N_K \sim 0.1$) at which the effects of long mean-free-paths and of multi-species effects on the yield trend are balanced. A more thorough exploration of N_K vs. f_D space would be valuable to identify this transition point.

In deuterium-tritium mixtures, which are the primary fuel mixture for efforts towards fusion ignition, the mean-free-path of the two species is more comparable: the deuteron mean-free-path λ_D is smaller than λ_T by a factor of $\sim$0.8. Because λ_D is smaller, the average mean-free-path and the Knudsen number decrease with increased deuterium fraction in DT when maintaining mass density. This trend is opposite of the trend in D^3He; as such, long mean-free-path effects and multi-species effects will both tend to reduce performance of DT mixtures relative to pure deuterium. However, because of the reduced magnitude of the N_K trend with f_D ($\sim$1/3$\times$ as compared to $\sim$10$\times$), deuterium-tritium mixtures better decouple the effects of long mean-free-paths from multi-species dynamics, making DT valuable for future physics studies.

The plasmas produced in this study are relevant to the shocked DT-vapor at the onset of deceleration in ICF experiments, for which $N_K \sim 0.2$–0.8.[3] While the nuclear yield at this phase of the experiment is negligible, the state of the central plasma is important in establishing the trajectory of deceleration for the cold fuel. Standard hydrodynamic methods assume the shocked vapor is isentropically compressed and heated by the ice layer, and heat flow from the core ablates cryogenic fuel from the inner surface to form the bulk of the hot spot mass. However the present work suggests that the distribution function of core ions is already far from Maxwellian: assuming mean-free-paths are $\sim$1/2 of the core radius implies $\sim$7/8 of the core volume is within one mean-free-path of the wall. In this scenario, hydrodynamic estimates of compressional heating and heat transport will not apply. Instead, free-streaming particles will rapidly deposit their kinetic energy in the cold fuel, or gain energy by reflection off the fuel without significantly reducing fuel velocity. This will continue until energy loss from the core or increased density from continuing compression and mass ablation reduce mean-free-paths to a point at which hydrodynamics regains validity. This kinetic process in the hotspot will change the initial conditions for fuel assembly and hotspot formation.

The impact of kinetic physics on hotspot formation as has been suggested by Vlasov Fokker Planck simulations,[5] and may contribute to the observed low areal densities and high ion temperatures of layered DT experiments at the NIF when compared to hydrodynamic predictions. Experimentally, this hypothesis can be tested by varying the Knudsen number of the initial DT vapor, which can be done using liquid DT layers.[37] Improved understanding of the kinetic dynamics of hotspot formation through Vlasov-Fokker-Planck or hybrid-PIC simulations will inform and support the continued use of hydrodynamic tools to design an igniting ICF implosion.

References

[1] W. H. Goldstein, "Science of Fusion Ignition on NIF," Tech. Rep. LLNL-TR-570412, Lawrence Livermore National Laboratory, May 2012.

[2] S. W. Haan, J. D. Lindl, D. A. Callahan, D. S. Clark, J. D. Salmonson, B. A. Hammel, L. J. Atherton, R. C. Cook, M. J. Edwards, S. Glenzer, A. V. Hamza, S. P. Hatchett, M. C. Herrmann, D. E. Hinkel, D. D. Ho, H. Huang, O. S. Jones, J. Kline, G. Kyrala, O. L. Landen, B. J. MacGowan, M. M. Marinak, D. D. Meyerhofer, J. L. Milovich, K. A. Moreno, E. I. Moses, D. H. Munro, A. Nikroo, R. E. Olson, K. Peterson, S. M. Pollaine, J. E. Ralph, H. F. Robey, B. K. Spears, P. T. Springer, L. J. Suter, C. A. Thomas, R. P. Town, R. Vesey, S. V. Weber, H. L. Wilkens, and D. C. Wilson, "Point design targets, specifications, and requirements for the 2010 ignition campaign on the National Ignition Facility," *Physics of Plasmas*, vol. 18, p. 051001, 2011.

[3] M. J. Rosenberg, A. B. Zylstra, F. H. Séguin, H. G. Rinderknecht, J. A. Frenje, M. Gatu Johnson, H. Sio, C. J. Waugh, N. Sinenian, C. K. Li, R. D. Petrasso, P. W. McKenty, M. Hohenberger, P. B. Radha, J. A. Delettrez, V. Y. Glebov, R. Betti, V. N. Goncharov, J. P. Knauer, T. C. Sangster, S. LePape, A. J. Mackinnon, J. Pino, J. M. McNaney, J. R. Rygg, P. A. Amendt, C. Bellei, L. R. Benedetti, L. Berzak Hopkins, R. M. Bionta, D. T. Casey, L. Divol, M. J. Edwards, S. Glenn, S. H. Glenzer, D. G. Hicks, J. R. Kimbrough, O. L. Landen, J. D. Lindl, T. Ma, A. MacPhee, N. B. Meezan, J. D. Moody, M. J. Moran, H.-S. Park, B. A. Remington, H. Robey, M. D. Rosen, S. C. Wilks, R. A. Zacharias, H. W. Herrmann, N. M. Hoffman, G. A. Kyrala, R. J. Leeper, R. E. Olson, J. D. Kilkenny, and A. Nikroo, "Investigation of ion kinetic effects in direct-drive exploding-pusher implosions at the nif," *Physics of Plasmas (1994-present)*, vol. 21, no. 12, 2014.

[4] C. Bellei, H. Rinderknecht, A. Zylstra, M. Rosenberg, H. Sio, C. K. Li, R. Petrasso, S. C. Wilks, and P. A. Amendt, "Species separation and kinetic effects in collisional plasma shocks," *Physics of Plasmas*, vol. 21, no. 5, p. 056310, 2014.

[5] A. Inglebert, B. Canaud, and O. Larroche, "Species separation and modification of neutron diagnostics in inertial-confinement fusion," *EPL (Europhysics Letters)*, vol. 107, no. 6, p. 65003, 2014.

[6] B. E. Peigney, O. Larroche, and V. Tikhonchuk, "Ion kinetic effects on the ignition and burn of inertial confinement fusion targets: A multi-scale approach," *Physics of Plasmas*, vol. 21, no. 12, pp. –, 2014.

[7] M. J. Rosenberg, H. G. Rinderknecht, N. M. Hoffman, P. A. Amendt, S. Atzeni, A. B. Zylstra, C. K. Li, F. H. Séguin, H. Sio, M. G. Johnson, J. A. Frenje, R. D. Petrasso, V. Y. Glebov, C. Stoeckl, W. Seka, F. J. Marshall, J. A. Delettrez, T. C. Sangster, R. Betti, V. N. Goncharov, D. D. Meyerhofer, S. Skupsky, C. Bellei, J. Pino, S. C. Wilks, G. Kagan, K. Molvig, and A. Nikroo, "Exploration of the Transition from the Hydrodynamiclike to the Strongly Kinetic Regime in Shock-Driven Implosions," *Physical Review Letters*, vol. 112, p. 185001, May 2014.

[8] K. Molvig, N. M. Hoffman, B. J. Albright, E. M. Nelson, and R. B. Webster, "Knudsen Layer Reduction of Fusion Reactivity," *Physical Review Letters*, vol. 109, p. 095001, Aug 2012.

[9] B. J. Albright, K. Molvig, C. K. Huang, A. N. Simakov, E. S. Dodd, N. M. Hoffman, G. Kagan, and P. F. Schmit, "Revised Knudsen-layer reduction of fusion reactivity," *Physics of Plasmas*, vol. 20, no. 12, p. 122705, 2013.

[10] G. Kagan, D. Svyatskiy, H. G. Rinderknecht, M. J. Rosenberg, A. B. Zylstra, C. K. Huang, and C. J. McDevitt, "Self-Similar Structure and Experimental Signatures of Suprathermal Ion Distribution in Inertial Confinement Fusion Implosions," *Physical Review Letters*, vol. 115, p. 105002, Sept. 2015.

[11] N. M. Hoffman, G. B. Zimmerman, K. Molvig, H. G. Rinderknecht, M. J. Rosenberg, B. J. Albright, A. N. Simakov, H. Sio, A. B. Zylstra, M. G. Johnson, F. H. Sguin, J. A. Frenje, C. K. Li, R. D. Petrasso, D. M. Higdon, G. Srinivasan, V. Y. Glebov, C. Stoeckl, W. Seka, and T. C. Sangster, "Approximate models for the ion-kinetic regime in inertial-confinement-fusion capsule implosions," *Physics of Plasmas (1994-present)*, vol. 22, no. 5, 2015.

[12] J. R. Rygg, J. A. Frenje, C. K. Li, F. H. Séguin, R. D. Petrasso, J. A. Delettrez, V. Y. Glebov, V. N. Goncharov, D. D. Meyerhofer, S. P. Regan, T. C. Sangster, and C. Stoeckl, "Tests of the hydrodynamic equivalence of direct-drive implosions with different D_2 and ^{3}He mixtures," *Physics of Plasmas*, vol. 13, no. 5, p. 052702, 2006.

[13] D. C. Wilson, G. A. Kyrala, J. F. B. Jr., F. J. Wysocki, M. A. Gunderson, W. J. Garbett, V. Y. Glebov, J. Frenje, B. Yaakobi, H. W. Herrman, J. H. Cooley, L. Welser-Sherrill, C. J. Horsfield, and S. A. Roberts, "The effects of pre-mix on burn in ICF capsules," *Journal of Physics: Conference Series*, vol. 112, p. 022015, 2008.

[14] H. W. Herrmann, J. R. Langenbrunner, J. M. Mack, J. H. Cooley, D. C. Wilson, S. C. Evans, T. J. Sedillo, G. A. Kyrala, S. E. Caldwell, C. S. Young, A. Nobile, J. Wermer, S. Paglieri, A. M. McEvoy, Y. Kim, S. H. Batha, C. J. Horsfield, D. Drew, W. Garbett, M. Rubery, V. Y. Glebov, S. Roberts, and J. A. Frenje, "Anomalous yield reduction in direct-drive deuterium/tritium implosions due to ^{3}He addition," *Physics of Plasmas*, vol. 16, no. 5, p. 056312, 2009.

[15] D. T. Casey, J. A. Frenje, M. Gatu Johnson, M. J.-E. Manuel, H. G. Rinderknecht, N. Sinenian, F. H. Séguin, C. K. Li, R. D. Petrasso, P. B. Radha, J. A. Delettrez, V. Y. Glebov, D. D. Meyerhofer, T. C. Sangster, D. P. McNabb, P. A. Amendt, R. N. Boyd, J. R. Rygg, H. W. Herrmann, Y. H. Kim, and A. D. Bacher, "Evidence for stratification of deuterium-tritium fuel in inertial confinement fusion implosions," *Physical Review Letters*, vol. 108, p. 075002, Feb 2012.

[16] H. G. Rinderknecht, M. J. Rosenberg, C. K. Li, N. M. Hoffman, G. Kagan, A. B. Zylstra, H. Sio, J. A. Frenje, M. Gatu Johnson, F. H. Séguin, R. D. Petrasso, P. Amendt, C. Bellei, S. Wilks, J. Delettrez, V. Y. Glebov, C. Stoeckl, T. C. Sangster, D. D. Meyerhofer, and A. Nikroo, "Ion thermal decoupling and species separation in shock-driven implosions," *Physical Review Letters*, vol. 114, p. 025001, Jan 2015.

[17] P. Amendt, O. Landen, H. Robey, C. Li, and R. Petrasso, "Plasma Barodiffusion in Inertial-Confinement-Fusion Implosions: Application to Observed Yield Anomalies in Thermonuclear Fuel Mixtures," *Physical Reviev Letters*, vol. 105, p. 115005, Sep 2010.

[18] P. Amendt, S. C. Wilks, C. Bellei, C. K. Li, and R. D. Petrasso, "The potential role of electric fields and plasma barodiffusion on the inertial confinement fusion database," *Physics of Plasmas*, vol. 18, no. 5, p. 056308, 2011.

[19] G. Kagan and X.-Z. Tang, "Electro-diffusion in a plasma with two ion species," *Physics of Plasmas*, vol. 19, no. 8, p. 082709, 2012.

[20] G. Kagan and X.-Z. Tang, "Thermo-diffusion in inertially confined plasmas," *Physics Letters A*, vol. 378, no. 21, p. 1531, 2014.

[21] P. Amendt, C. Bellei, S. Wilks, C. K. Li, R. D. Petrasso, and H. G. Rinderknecht, "Shock-driven resistive heating in mixed species thermonuclear fuels," *Physical Review E*, (to be submitted).

[22] T. R. Boehly, D. L. Brown, R. S. Craxton, R. L. Keck, J. P. Knauer, J. H. Kelly, T. J. Kessler, S. A. Kumpan, S. J. Loucks, S. A. Letzring, F. J. Marshall, R. L. McCrory, S. F. B. Morse, W. Seka, J. M. Soures, and C. P. Verdon, "Initial performance results of the OMEGA laser system," *Optics Communications*, vol. 133, no. 1-6, p. 495, 1997.

[23] V. Y. Glebov, C. Stoeckl, T. C. Sangster, S. Roberts, G. J. Schmid, R. A. Lerche, and M. J. Moran, "Prototypes of National Ignition Facility neutron time-of-flight detectors tested on OMEGA," *Review of Scientific Instruments*, vol. 75, no. 10, p. 3559, 2004.

[24] F. H. Séguin, J. A. Frenje, C. K. Li, D. G. Hicks, S. Kurebayashi, J. R. Rygg, B. E. Schwartz, R. D. Petrasso, S. Roberts, J. M. Soures, D. D. Meyerhofer, T. C. Sangster, J. P. Knauer, C. Sorce, V. Y. Glebov, C. Stoeckl, T. W. Phillips, R. J. Leeper, K. Fletcher, and S. Padalino, "Spectrometry of charged particles from inertial-confinement-fusion plasmas," *Review of Scientific Instruments*, vol. 74, no. 2, p. 975, 2003.

[25] H. Brysk, "Fusion neutron energies and spectra," *Plasma Physics*, vol. 15, p. 611, July 1973.

[26] L. Ballabio, J. Källne, and G. Gorini, "Relativistic calculation of fusion product spectra for thermonuclear plasmas," *Nuclear Fusion*, vol. 38, no. 11, p. 1723, 1998.

[27] F. H. Séguin, J. L. DeCiantis, J. A. Frenje, C. K. Li, J. R. Rygg, C. D. Chen, R. D. Petrasso, J. A. Delettrez, S. P. Regan, V. A. Smalyuk, V. Y. Glebov, J. P. Knauer, F. J. Marshall, D. D. Meyerhofer, S. Roberts, T. C. Sangster, C. Stoeckl, K. Mikaelian, H. S. Park, H. F. Robey, and R. E. Tipton, "Measured dependence of nuclear burn region size on implosion parameters in inertial confinement fusion experiments," *Physics of Plasmas*, vol. 13, no. 8, p. 082704, 2006.

[28] D. K. Bradley, P. M. Bell, O. L. Landen, J. D. Kilkenny, and J. Oertel, “Development and characterization of a pair of 30-40 ps x-ray framing cameras,” *Review of Scientific Instruments*, vol. 66, no. 1, p. 716, 1995.

[29] J. T. Larsen and S. M. Lane, “HYADES - A plasma hydrodynamics code for dense plasma studies,” *Journal of Quantitative Spectroscopy and Radiative Transfer*, vol. 51, p. 179, 1994.

[30] W. Seka, H. A. Baldis, J. Fuchs, S. P. Regan, D. D. Meyerhofer, C. Stoeckl, B. Yaakobi, R. S. Craxton, and R. W. Short, “Multibeam Stimulated Brillouin Scattering from Hot, Solid-Target Plasmas,” *Physical Review Letters*, vol. 89, no. 17, p. 175002, 2002.

[31] R. A. Lerche, D. W. Phillion, and G. L. Tietbohl, “25 ps neutron detector for measuring ICF-target burn history,” *Review of Scientific Instruments*, vol. 66, no. 1, p. 933, 1995.

[32] J. A. Frenje, C. K. Li, F. H. Séguin, J. Deciantis, S. Kurebayashi, J. R. Rygg, R. D. Petrasso, J. Delettrez, V. Y. Glebov, C. Stoeckl, F. J. Marshall, D. D. Meyerhofer, T. C. Sangster, V. A. Smalyuk, and J. M. Soures, “Measuring shock-bang timing and ρR evolution of D^3He implosions at OMEGA,” *Physics of Plasmas*, vol. 11, no. 5, p. 2798, 2004.

[33] M. J. May, K. Widmann, C. Sorce, H.-S. Park, and M. Schneider, “Uncertainty analysis technique for OMEGA Dante measurements,” *Review of Scientific Instruments*, vol. 81, no. 10, 2010.

[34] H. G. Rinderknecht, M. G. Johnson, A. B. Zylstra, N. Sinenian, M. J. Rosenberg, J. A. Frenje, C. J. Waugh, C. K. Li, F. H. Sguin, R. D. Petrasso, J. R. Rygg, J. R. Kimbrough, A. MacPhee, G. W. Collins, D. Hicks, A. Mackinnon, P. Bell, R. Bionta, T. Clancy, R. Zacharias, T. Döppner, H. S. Park, S. LePape, O. Landen, N. Meezan, E. I. Moses, V. U. Glebov, C. Stoeckl, T. C. Sangster, R. Olson, J. Kline, and J. Kilkenny, “A novel particle time of flight diagnostic for measurements of shock- and compression-bang times in D^3He and DT implosions at the NIF,” *Review of Scientific Instruments*, vol. 83, no. 10, pp. –, 2012.

[35] M. D. Cable and S. P. Hatchett, “Neutron spectra from inertial confinement fusion targets for measurement of fuel areal density and charged particle stopping powers,” *Journal of Applied Physics*, vol. 62, no. 6, pp. 2233–2236, 1987.

[36] F. H. Séguin, C. K. Li, J. A. Frenje, D. G. Hicks, K. M. Green, S. Kurebayashi, R. D. Petrasso, J. M. Soures, D. D. Meyerhofer, V. Y. Glebov, P. B. Radha, C. Stoeckl, S. Roberts, C. Sorce, T. C. Sangster, M. D. Cable, K. Fletcher, and S. Padalino, “Using secondary-proton spectra to study the compression and symmetry of deuterium-filled capsules at OMEGA,” *Physics of Plasmas*, vol. 9, no. 6, p. 2725, 2002.

[37] R. E. Olson and R. J. Leeper, "Alternative hot spot formation techniques using liquid deuterium-tritium layer inertial confinement fusion capsules," *Physics of Plasmas*, vol. 20, no. 9, p. 092705, 2013.

This work performed under the auspices of the U.S. Department of Energy by Lawrence Livermore National Laboratory under Contract DE-AC52-07NA27344